


Models of continuous-time networks with tie decay, diffusion, and convectionXinzhe Zuo and Mason A. Porter *Department of Mathematics, University of California, Los Angeles, California 90095, USA* (Received 22 June 2019; revised 26 September 2020; accepted 28 October 2020; published 5 February 2021; corrected 8 April 2021)

The study of temporal networks in discrete time has yielded numerous insights into time-dependent networked systems in a wide variety of applications. However, for many complex systems, it is useful to develop continuous-time models of networks and to compare them to associated discrete models. In this paper, we study several continuous-time network models and examine discrete approximations of them both numerically and analytically. To consider continuous-time networks, we associate each edge in a graph with a time-dependent tie strength that can take continuous non-negative values and decays in time after the most recent interaction. We investigate how the moments of the tie strength evolve with time in several models, and we explore—both numerically and analytically—criteria for the emergence of a giant connected component in some of these models. We also briefly examine the effects of the interaction patterns of continuous-time networks on the contagion dynamics of a susceptible–infected–recovered model of an infectious disease.

DOI: [10.1103/PhysRevE.103.022304](https://doi.org/10.1103/PhysRevE.103.022304)**I. INTRODUCTION**

Networks, in the form of graphs or more complicated structures, are useful models of many complex systems in nature, society, and technology [1,2]. In the simplest case of a time-independent graph, one models entities as nodes and interactions between them as (possibly weighted and/or directed) edges. However, most networks change in time, and the study of temporal networks—in which nodes and/or edges change in time—is one of the most active areas of network science [3–5].

Temporal networks differ from time-independent networks in several respects. One significant feature is that the edges of a temporal network may change between active and inactive states. For example, in a communication network, e-mails or text messages are instantaneous interactions between entities, and we consider an edge between two entities to be active during instantaneous communication. In other situations, such as in a phone call, interactions between entities of a social network may be active for some finite duration of time. Temporal networks are very popular for studying time-dependent networked systems, but almost all formulations of them have focused on discrete time [6]. However, it is more appropriate to study many systems using continuous-time temporal networks, which allow both discrete and continuous ties. Indeed, even when interactions are instantaneous, their importance or influence may last beyond the interaction time itself, and one can model them as decaying continuously as a function of time [7–9]. In such a “tie-decay network” framework, as advocated in [6], one separates the concepts of interactions and ties between entities. An interaction may or may not be instantaneous (depending on the model), but the existence and weights of the ties—which are affected by the interactions—change continuously in time.

Ties between entities of a social network strengthen with repeated interactions, and they often deteriorate without such interactions [7,10]. Our paper is motivated by the recent for-

malization of tie-decay networks by Ahmad *et al.* [6]. In their study, the strength of a tie between nodes decays exponentially in the absence of interactions and discrete interactions between entities boost the strength of a tie between entities. This mechanism is also reminiscent of models of Hebbian learning in neuronal networks, as the tie strength between neurons can increase when they have similar interaction patterns [11]. In a 2001 paper on tie-decay networks (although without introducing such terminology), Jin *et al.* [12] examined continuous-time networks with an exponential decay of tie strengths that they used to represent friendship strengths between people in a social network. As we discuss in the present paper, there are various ways to formulate models of tie-decay networks, and we consider a few of them. Another approach for studying temporal networks in both continuous and discrete time is through statistical models, such as exponential random-graph models [13].

As discussed in [6], a major challenge of studying continuous-time temporal networks is the aggregation of interactions between entities over time windows. There is a delicate balance between smoothing noise and preserving information content, and the choice of the size of a time window plays an important role. If a time window is too small, one may be unable to capture some important features of a network. However, if the time window is too large, it may eclipse important interactions in a network. Given these issues, Sulo *et al.* illustrated that it is important to examine multiple resolutions in time-dependent networks [14]. In the present paper, we focus on the decay and boosting behavior of ties between pairs of nodes. Therefore, it is often more meaningful to examine the time step and the decay rate together, instead of studying them separately.

To improve the understanding of continuous-time networks, it is important to generalize well-known network models to continuous-time settings. An important example is Erdős–Rényi (ER) networks [1,15], the simplest type of ran-

dom graph. Each edge in a $G(n, p)$ ER graph exists with a homogeneous, independent probability p . An important feature of the $G(n, p)$ model is the emergence of a giant connected component (GCC), which scales linearly with the number n of nodes in a network, for probabilities that are at least some critical value [1,15]. A related idea, which has been used in models of numerous phenomena, is percolation on ER graphs and other networks [16]. Many scholars have studied GCCs (and giant percolating components) in a diverse set of applications, such as navigability in transportation networks [17] and transmissibility of diseases in social networks [18]. For example, Jin *et al.* [12] examined the development of a GCC in a model of the formation of a social network.

In the present paper, we incorporate the $G(n, p)$ model into several continuous-time network models using a variety of different mechanisms for the growth and decay of the tie strengths between nodes. These mechanisms include the tie-decay model of Ahmad *et al.* [6] and the back-to-unity model of Jin *et al.* [12]. We also study two mechanisms—a diffusion model and a convection–diffusion model—that are inspired by random walks and partial differential equations (PDEs). For all four of these mechanisms, we assume that the tie strength between a pair of nodes is independent of the tie strengths of any other edges in a network. With this independence assumption, we derive the moments of the tie strength at stationarity for the model of Ahmad *et al.* and a simplified version of the model of Jin *et al.*, and we then compare our results for the first moment with numerical simulations. We also study the emergence of a GCC in a simplified version of the back-to-unity model, the convection–diffusion model, and a particular limit of the tie-decay model of Ahmad *et al.* Our results give insights into several different types of continuous-time networks with tie decay, and we see that their properties can differ from each other in substantive ways. As a case study, we also briefly examine the effects of interaction patterns of the back-to-unity model on contagion dynamics in a susceptible–infected–recovered (SIR) model of an infectious disease.

Our paper proceeds as follows. In Sec. II, we discuss four models of continuous-time networks with tie decay: the recent model of Ahmad *et al.* [6], the back-to-unity model of Jin *et al.* [12], a diffusion model, and a convection–diffusion model. We examine the moments of tie strength in the Ahmad *et al.* model in the long-time limit. We also study the emergence of a GCC in a particular limit and compare it with our numerical simulations. We then study the moments of the tie strength and the emergence of a GCC in a simplified version of the back-to-unity model. We also introduce two continuous-time network models that are based on random walks—a diffusion model and a convection–diffusion model—and we examine the emergence of a GCC in our convection–diffusion network model using ideas from PDEs and numerical analysis. In Sec. III, we examine SIR dynamics on networks that we construct from a simplified version of the back-to-unity model. In Sec. IV, we summarize our results and suggest several future directions.

II. MODELS

A. Tie-decay model of Ahmad *et al.* [6]

We start with the tie-decay model of Ahmad *et al.* [6]. This graph model $G(n, p, \alpha, T)$ has four parameters: the number

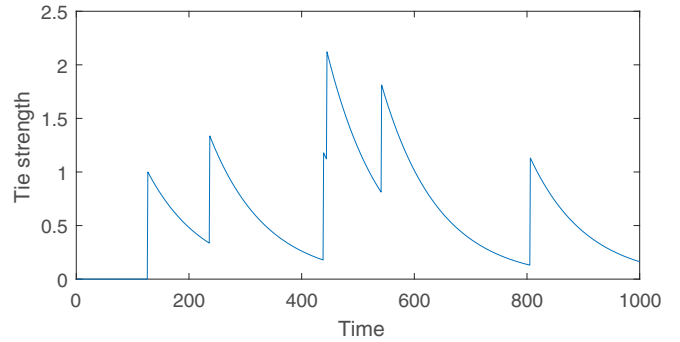


FIG. 1. An illustration of dynamics in the tie-decay model of Ahmad *et al.* [6]. The tie strength between a pair of nodes increases by 1 when there is an interaction during a time step, and it decays exponentially when there is no interaction. In the depicted simulation, there are $n = 1000$ nodes, a decay rate of $\alpha = 0.01$, an interaction probability of $p = 0.003$, and $T = 1000$ time steps. The vertical axis shows the tie strength of one edge. Six interactions occur between the two nodes that are incident to this edge.

n of nodes, the computation time (i.e., the number of time steps) T , a decay parameter α , and the probability p that a pair of nodes interacts during one time step. One considers the interaction probability p independently for each pair of nodes. This model distinguishes between the concepts of “interactions” and “ties,” which traditionally are treated as equivalent concepts. There is an underlying continuous time, which we measure in small increments of length δt , and a pair of nodes can interact during a time step. The strength of a tie between two nodes depends on the history of the interactions between them. The primary goal of [6] was to generalize PageRank centrality [19] to tie-decay networks. When we examine such tie-decay networks, we consider networks with undirected edges and tie strengths. We focus on the situation in which nodes in a network have an equal probability of interacting with any of the other nodes in each time step. Using a characteristic function, we derive the moments of the tie strength in the long-time limit. We also examine the criterion for the emergence of a GCC in a tie-decay network in the special case in which each node pair interacts at most once.

There are numerous possible choices in the above tie-decay setting, and we follow those of [6]. Consider a time step of length δt . If a pair of nodes interacts, which occurs with a homogeneous probability p , the tie strength of the edge between these nodes increases by 1. If they do not interact, which occurs with complementary probability $1 - p$, the strength of the tie between them decays by the factor $e^{-\alpha \delta t}$. We also make the assumption that, during a single time step, a pair of nodes either has one interaction (thereby increasing the strength of the tie between them) or has zero interactions (such that the tie strength between them decays). We suppose that the growth and decay pattern of each pair of nodes is independent of all other pairs, so we independently consider each node pair during each time step. As we mentioned in Sec. I, it is more appropriate to examine the time step and the decay rate together, rather than separately. For simplicity, we take $\delta t = 1$ in this model (and also in the back-to-unity model, which we discuss in Sec. II B). In Fig. 1, we show an example of the tie-decay model’s dynamics.

Let \mathbf{A} be an adjacency matrix that is associated with a graph from $G(n, p, \alpha, T)$ and encodes the tie strengths of the edges. The entry \mathbf{A}_{ef} gives the tie strength between nodes e and f (where $e \neq f$). The matrix \mathbf{A} is symmetric and has 0 entries on the diagonal.

The tie strength of each edge satisfies the same probability distribution, so let us focus on a single edge. Let s_t be the tie strength of a particular edge at time t , and suppose that $s_0 = 0$. To study the model of [6] with $\delta t = 1$, we run a Monte Carlo simulation for a total of T steps using the following update rule:

$$s_{t+1} = \begin{cases} s_t + 1, & \text{with probability } p \\ s_t e^{-\alpha}, & \text{with probability } (1 - p). \end{cases} \quad (1)$$

That is,

$$s_{t+1} = z_t + e^{-\alpha(1-z_t)} s_t,$$

where z_t is a Bernoulli random variable with parameter p .

To calculate the expectation of s_t , we write

$$\begin{aligned} \mathbb{E}[s_0] &= 0, \\ \mathbb{E}[s_1] &= p(1 + \mathbb{E}[s_0]) + e^{-\alpha} \mathbb{E}[s_0](1 - p), \\ &\vdots \\ \mathbb{E}[s_t] &= p(1 + \mathbb{E}[s_{t-1}]) + e^{-\alpha} \mathbb{E}[s_{t-1}](1 - p), \text{ for } t \geq 1. \end{aligned}$$

It is difficult to evaluate the above recursive expression to obtain a closed-form expression for $\mathbb{E}[s_t]$, but we can obtain a good approximation for large t . The expression for $\mathbb{E}[s_t]$ is a sum of terms of the form $p^i e^{-j\alpha}$, where $i \in \{1, \dots, t\}$ and $j \in \{0, \dots, t-1\}$. The coefficients of $p^i e^{-j\alpha}$ are all equal to 1 when $i + j \leq t$, and we can discard the other terms as small as $t \rightarrow \infty$. This allows us to approximate $\mathbb{E}[s_t]$ as follows:

$$\begin{aligned} \mathbb{E}[s_t] &\approx \sum_{i=1}^t \sum_{j=0}^{t-i} p^i e^{-j\alpha} \\ &= \frac{1}{1-\sigma} \left[\frac{p - p^{t+1}}{1-p} - p\sigma^t \left(\frac{\left(\frac{p}{\sigma}\right)^t - 1}{\frac{p}{\sigma} - 1} \right) \right], \end{aligned} \quad (2)$$

where $\sigma = e^{-\alpha}$. This also yields the long-time behavior of $\mathbb{E}[s_t]$, which is given by

$$\lim_{t \rightarrow \infty} \mathbb{E}[s_t] = \frac{1}{1-\sigma} \frac{p}{1-p}. \quad (3)$$

In the long-time limit, which is a stationary state, we can write down the characteristic function of the distribution of $s := \lim_{t \rightarrow \infty} s_t$. This function is

$$\phi_s(k) = \mathbb{E}[e^{iks}], \quad (4)$$

where $i^2 = -1$. From the tie-decay interaction and assuming that the system is in a stationary state, it follows that

$$\phi_s(k) = p e^{ik} \phi_s(k) + (1-p) \phi_s(\sigma k). \quad (5)$$

We do not possess a closed-form solution to Eq. (5). However, we can obtain all of the moments of s by differentiating Eq. (5) and using the initial condition $\phi_s(0) = 1$. The m th derivative

of ϕ_s at $k = 0$ is

$$\phi_s^{(m)}(0) = \frac{p \left[\sum_{j=1}^m \binom{m}{j} \phi_s^{(m-j)}(0) i^j \right]}{(1-p)(1-\sigma^m)}, \quad (6)$$

where $\phi_s^{(j)}(0)$ is the j th derivative of ϕ_s evaluated at 0. Using Eq. (6), we calculate the mean $\mathbb{E}[s]$ and variance $\text{var}(s)$ of s to be

$$\begin{aligned} \mathbb{E}[s] &= \frac{p}{(1-\sigma)(1-p)}, \\ \text{var}(s) &= \frac{p}{(1-\sigma^2)(1-p)^2}. \end{aligned}$$

We thereby recover Eq. (3).

We now verify that we indeed reach a stationary state as $t \rightarrow \infty$. The map with $x \mapsto [p(x+1) + (1-p)\sigma x]$ is a contraction when $\alpha > 0$ and $p < 1$. Let $x, y \in \mathbb{R}$ and $\phi(x) = [p(x+1) + (1-p)\sigma x]$. It then follows that

$$\begin{aligned} |\phi(x) - \phi(y)| &= |p(x-y) + (1-p)\sigma(x-y)| \\ &\leq |x-y| [p + (1-p)\sigma]. \end{aligned}$$

By the Banach fixed-point theorem, we achieve a stationary state by iteration.

We now examine how well Eqs. (2) and (3) agree using direct numerical simulations of tie-decay networks. Our networks have $n = 3000$ nodes, a connection probability of $p = 0.1$, and a decay rate of $\alpha = 0.05$. Equation (3) yields a limiting expectation value of 2.2782. At $t = 50$, our numerical computations yield $\mathbb{E}[s_t] \approx 2.0368$ and our analytical approximation (2) yields 2.0902; at $t = 100$, we calculate that $\mathbb{E}[s_t] \approx 2.2524$ and our analytical approximation yields 2.2628; at $t = 150$, we calculate that $\mathbb{E}[s_t] \approx 2.2751$ and our analytical approximation yields 2.2770; at $t = 500$, we calculate that $\mathbb{E}[s_t] \approx 2.2782$ and our analytical approximation yields 2.2782.

As t becomes larger, our simulations and approximation become progressively closer to each other. The approximation is always larger than our simulation results because the coefficients of the largest terms ($p^i e^{-j\alpha}$ with $i + j = t + 1$) that we dropped in our approximation are always negative. If we include terms of this order in our sum, our refined approximation is smaller than our simulation results because the coefficients of the next-largest terms ($p^i e^{-j\alpha}$ with $i + j = t + 2$) in the sum are always positive. Based on our numerical computations, we observe that these positive and negative corrections to our approximation balance each other, rendering Eq. (3) an accurate approximation in the long-time limit.

As we noted previously, we do not possess closed-form expressions for the stationary distribution of the tie strengths or for its characteristic function (5). However, by reformulating the problem as a Poisson process for large T and small p , we can approximate the stationary distribution of the tie strength in the special case in which each node pair interacts at most once.

Consider a Poisson process with mean and variance $\lambda = Tp$. The tie strength decays exponentially in time until the Poisson process experiences an arrival, which causes the tie strength to increase instantaneously by 1. This is an equivalent formulation of the tie-decay process with a total simulation time of T . The number N_T of arrivals over time T for the

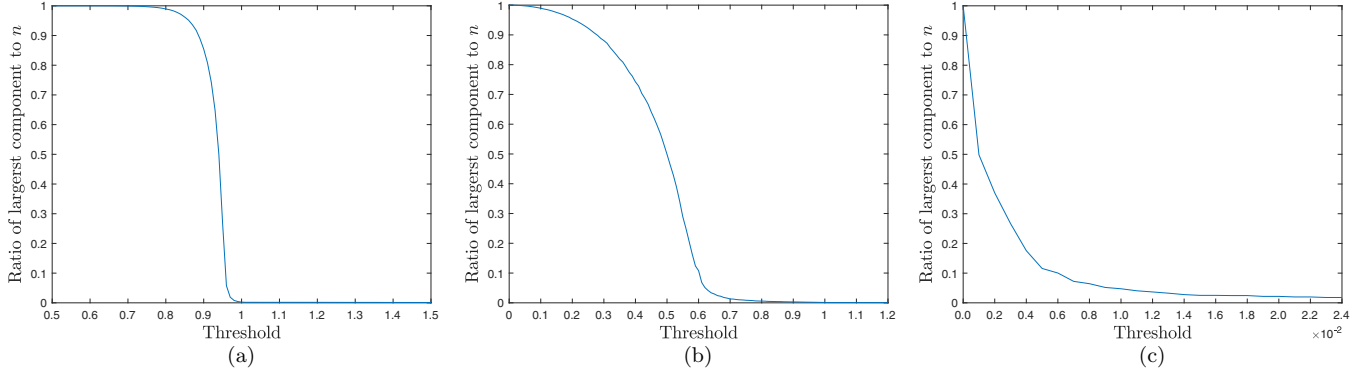


FIG. 2. Size of the largest connected component in a tie-decay network that we construct using the model of Ahmad *et al.* [6] versus the threshold g for different values of the decay rate α . In our simulations, there are $n = 2000$ nodes; decay parameters of (a) $\alpha = 0.001$, (b) $\alpha = 0.01$, and (c) $\alpha = 0.1$; a total simulation time of $T = 1000$; and an interaction probability of $p = 10^{-5}$ (so $\lambda = Tp = 0.01$). Each plot is a mean over 200 instantiations. Using Eq. (13), we calculate the critical thresholds g_{crit} to be (a) 0.9592, (b) 0.6345, and (c) 0.0106.

Poisson process follows the Poisson distribution

$$\mathbf{P}(N_T = j) = \frac{\lambda^j \exp(-\lambda)}{j!}. \quad (7)$$

Let s be the tie strength of an edge at the end (specifically, with $t \rightarrow \infty$) of a tie-decay process that starts at $s_0 \geq 0$. By the law of total probability,

$$\mathbf{P}(s < \tilde{s}) = \sum_{j=0}^{\infty} \mathbf{P}(s < \tilde{s} | N_T = j) \mathbf{P}(N_T = j). \quad (8)$$

The case in which $N_T = 0$ is not very interesting, as the tie strength just decays exponentially. When $N_T = 1$, let τ be the (unique) arrival time of the Poisson process. If $\tilde{s} \geq (s_0 + 1) \exp(-T\alpha)$ (where equality holds when the arrival occurs at $t = 0$), it follows that

$$\{s < \tilde{s}\} \iff \left\{ \tau < \frac{1}{\alpha} \ln(\tilde{s} \exp(T\alpha) - s_0) \right\}. \quad (9)$$

The logical statement (9) suggests that we can readily calculate the distribution of τ , as there is a unique arrival during the interval. It follows that

$$\mathbf{P}(\tau \leq t | N_T = 1) = \frac{t}{T}. \quad (10)$$

From (9) and (10), we obtain

$$\mathbf{P}(s < \tilde{s} | N_T = 1) = \begin{cases} \frac{\ln(\tilde{s} e^{T\alpha} - s_0)}{\alpha T}, & \tilde{s} \geq (s_0 + 1) e^{-T\alpha} \\ 0, & \text{otherwise.} \end{cases} \quad (11)$$

When $\lambda \ll 1$, we can approximate the tie-decay process by assuming that $\mathbf{P}(N_T \geq 2) = 0$. That is, we are assuming that each node forms at most one tie during the entire process. In this scenario, suppose that $\tilde{s} \geq (s_0 + 1) \exp(-T\alpha)$. It then follows that

$$\begin{aligned} \mathbf{P}(s < \tilde{s}) &\approx \sum_{j=0}^1 \mathbf{P}(s < \tilde{s} | N_T = j) \mathbf{P}(N_T = j) \\ &= e^{-Tp} \left[1 + \frac{p}{\alpha} \ln(\tilde{s} e^{T\alpha} - s_0) \right]. \end{aligned} \quad (12)$$

We now impose a threshold g for the tie strength, such that we only consider edges with tie strengths that are at least g to be active.

Setting $\tilde{s} = g$, we approximate the value of a critical threshold g_{crit} for the emergence of a GCC in a tie-decay network. We write

$$g_{\text{crit}} = \exp \left\{ \frac{\alpha}{p} \left[e^{Tp} \left(1 - \frac{1}{n} \right) - 1 \right] - T\alpha \right\} + s_0 e^{-T\alpha}. \quad (13)$$

If $g < g_{\text{crit}}$, there is a GCC in our tie-decay network with high probability (i.e., with a probability that approaches 1 as $n \rightarrow \infty$); if $g > g_{\text{crit}}$, then with high probability there is not a GCC. In Fig. 2, we examine the effect of the decay parameter α on g_{crit} . We calculate that the critical thresholds g_{crit} for a GCC to emerge are $g_{\text{crit}} \approx 0.9502$, $g_{\text{crit}} \approx 0.6345$, and $g_{\text{crit}} \approx 0.0106$ for decay rates of $\alpha = 0.001$, $\alpha = 0.01$, and $\alpha = 0.1$, respectively. In our simulations, we observe a phase transition near $g = g_{\text{crit}}$.

B. A simplified version of the back-to-unity model of Jin *et al.* [12]

Jin *et al.* [12] considered a type of tie-decay model (although they did not use that terminology) in which an interaction resets the strength of a tie between two nodes to 1, instead of increasing the tie strength by 1 [as in Eq. (1)]. Consequently, the tie strength of each edge is always bounded above by 1. In Fig. 3, we show an illustrative example of the tie-decay dynamics for the back-to-unity model of [12].

In their back-to-unity model, Jin *et al.* [12] used a threshold $g \in (0, 1]$ for the tie strength and they interpreted edges with a tie strength of at least g as active. They examined the evolution of model friendship networks using numerical simulations. The main assumption in [12] is that two people are more likely to meet when they have common friends than when they do not. Each time two people meet, the tie strength of the edge between them resets to 1. When they are apart, the tie strength between them decreases exponentially. Jin *et al.* also included an upper bound for the number of active friends that one person can have simultaneously. Using their model, they sought to achieve insights into the formation of social

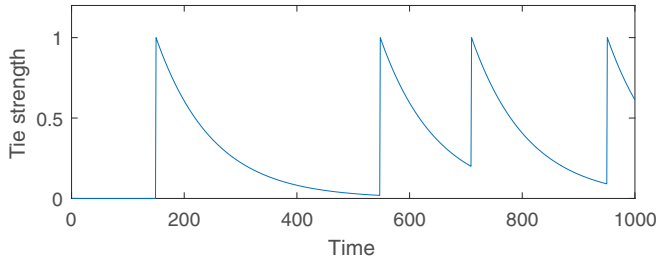


FIG. 3. An illustration of tie-decay dynamics in a simplified version of the back-to-unity model of Jin *et al.* [12]. The tie strength between two nodes resets to 1 if they interact during a time step. In the depicted simulation, there are $n = 1000$ nodes, a decay rate of $\alpha = 0.01$, an interaction probability of $p = 0.003$, and $T = 1000$ time steps. The vertical axis shows the tie strength of one edge. Four interactions occur between the two nodes that are incident to this edge.

networks, and they supposed that a community forms in a network concomitantly with the formation of a GCC.

In our discussion, we modify (and simplify) the back-to-unity model of [12] by dropping (1) the assumption that the chance that two people meet each other depends on the number of their mutual friends and (2) the upper bound on the number of friendships. With this simplified model, we can make some analytical progress. Given an interaction probability p and a threshold g , we derive a closed-form expression for the criterion of the emergence of a GCC.

The long-time behavior of the m th moment of the tie strength is

$$\lim_{t \rightarrow \infty} \mathbb{E}[s_t^m] = \frac{p}{1 - \sigma^m(1 - p)}, \quad (14)$$

where we recall that $\sigma = e^{-\alpha}$.

In the time-independent ER random-graph model $G(n, p)$, there is a GCC with high probability when

$$p \geq \frac{1 + \varepsilon}{n} \quad (15)$$

for any $\varepsilon > 0$, because there is a phase transition for the emergence of the GCC when $\varepsilon = 0$. When (15) holds, then with high probability, there is a single GCC and all other components have size $O(\ln(n))$ [15].

Because the nodes are indistinguishable from each other, we examine the probability that the strength of a particular edge is at least as large as the threshold:

$$\mathbf{P}(s \geq g) = 1 - \mathbf{P}(s < g), \quad (16)$$

where we recall that $s = \lim_{t \rightarrow \infty} s_t$. We compute the probability on the right-hand side of (16) as follows. We know that s cannot reset to 1 in the last step, as otherwise $s = 1 \geq g$. Similarly, s cannot reset to 1 in the last q steps, because otherwise it will not have enough time to decay to some value that is smaller than g . Using this argument, we see that q needs to satisfy

$$e^{-\alpha q} < g,$$

which implies that

$$q \geq \left\lceil -\frac{\ln(g)}{\alpha} \right\rceil,$$

where $\lceil \theta \rceil$ is the ceiling function of θ (i.e., the smallest integer that is at least as large as θ) and we have assumed that $\ln(g)/\alpha$ is not an integer.¹ The probability that s does not reset to 1 in the last q steps is $(1 - p)^q$, so

$$\begin{aligned} \mathbf{P}(s \geq g) &= 1 - \mathbf{P}(s < g) \\ &= 1 - (1 - p)^{\lceil -\ln(g)/\alpha \rceil}. \end{aligned} \quad (17)$$

By the same argument, a GCC exists with high probability if

$$\mathbf{P}(s \geq g) = 1 - (1 - p)^{\lceil -\ln(g)/\alpha \rceil} > \frac{1}{n}. \quad (18)$$

¹When $\ln(g)/\alpha$ is an integer, $e^{-\alpha q} \leq g$ instead of having a strict inequality.

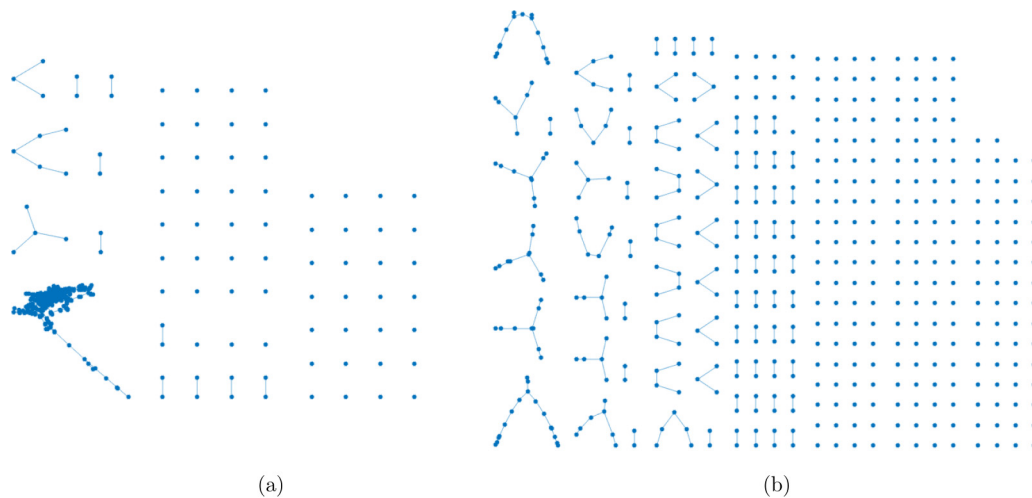


FIG. 4. Presence versus absence of a GCC in the simplified back-to-unity model. In each panel, we show all components of a network from a single simulation. In both simulations, there are $n = 1000$ nodes, an interaction probability of $p = \frac{1}{1.1n}$, a decay parameter of $\alpha = 0.01$, and $T = 3000$ time steps. (a) We set the threshold to be $g = 0.95$, which yields $\mathbf{P}(s \geq g) \approx 0.0054 > 1/n = 0.001$. Therefore, there is a GCC with high probability. (b) We set the threshold to be $g = 0.995$, which yields $\mathbf{P}(s \geq g) \approx 9.09 \times 10^{-4} < 1/n = 0.001$. Therefore, with high probability, there is no GCC.

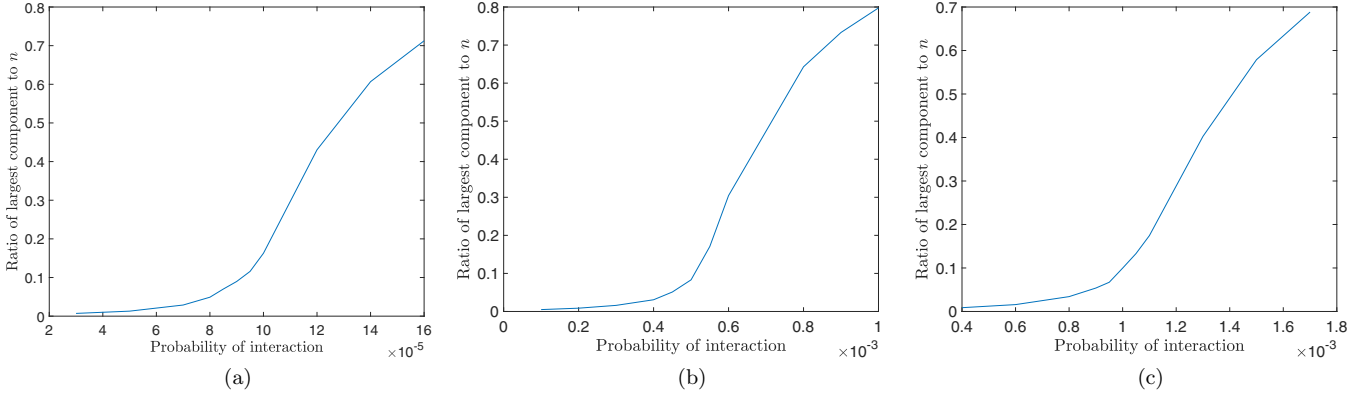


FIG. 5. Size of the largest connected component in networks that we construct using the simplified back-to-unity model. In our simulations, there are $n = 1000$ nodes; a decay parameter of (a) $\alpha = 0.01$, (b) $\alpha = 0.1$, and (c) $\alpha = 1$; and a threshold of $g = 0.9$. For each value of the interaction probability p , we take a mean of our results over 250 realizations. Each realization has a run time of $T = 500$. Using Eq. (18), we calculate the critical probabilities p_{crit} to be (a) 9×10^{-5} , (b) 0.5×10^{-3} , and (c) 1×10^{-3} .

Because $g \in (0, 1]$ and the decay parameter is $\alpha > 0$, it follows that $[-\ln(g)/\alpha] > 0$. Therefore, if $p > 1/n$, there is a GCC with high probability unless $g = 1$. That is, $p > 1/n$ is a sufficient condition for the existence of a GCC with high probability. Recall that this is also the condition for the existence of a GCC in Eq. (15). Therefore, the criterion for the existence of a GCC in a network that one constructs from the simplified back-to-unity model is stricter than that for an ordinary ER $G(n, p)$ graph. In Fig. 4, we illustrate the presence and absence of a GCC in a network with back-to-unity interactions. Our analytical result in Eq. (18) agrees with our numerical computations.

We also investigate numerically how the size of the GCC (if there is one) in a network that we construct from the simplified back-to-unity model varies with the interaction probability p when we fix all other parameters. We show the results of our numerical computations in Fig. 5. Based on Eq. (18) and our parameter values, we calculate that the critical probabilities p_{crit} for a GCC to emerge are $p_{\text{crit}} \approx 9 \times 10^{-5}$, $p_{\text{crit}} \approx 0.5 \times 10^{-3}$, and $p_{\text{crit}} \approx 1 \times 10^{-3}$ for decay rates of $\alpha = 0.01$,

$\alpha = 0.1$, and $\alpha = 1$, respectively. As we see in our simulations, there is a phase transition near $p = p_{\text{crit}}$.

C. Diffusion model of tie strengths

Another continuous-time model, which we introduce in the present paper, is a toy model of a tie-decay network based on diffusion. At each time step, each entity is equally likely to interact with some entity or to not do anything. Each interaction that occurs between a pair of nodes is independent of all other pairs (i.e., all other edges), so the strength of each tie changes independently of all other ties. This implies that, at each time step, there is an equal probability (of $1/2$) for the tie strength of each edge to grow or decay by the factor $\exp(\delta x)$ for some δx , which we assume is small. We assume that the tie strength of each edge starts at $\exp(0) = 1$. See Fig. 6(a) for an illustration of the dynamics of this diffusion model. We show that we can approximate the evolution of the distribution of tie strengths by a linear diffusion equation, as in the derivation of a diffusion equation from a symmetric random walk. In

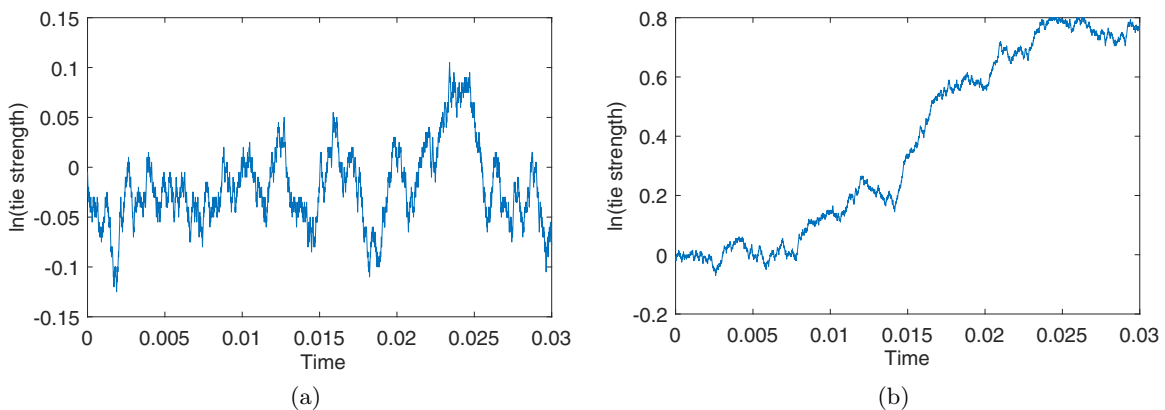


FIG. 6. An illustration of tie-strength dynamics for (a) our diffusion model and (b) our bounded convection–diffusion model. In both panels, we use a spatial step of $\delta x = 5 \times 10^{-3}$, a time step of $\delta t = 10^{-5}$, and a simulation time of $T = 0.03$. For panel (b), the convection parameter is $\beta = 5$ and the upper bound of the tie strength is $w = 0.8$. The vertical axis of each panel gives the natural logarithm of the tie strength of a single edge. In contrast to our simulations of the Ahmad *et al.* tie-decay model and the simplified back-to-unity model, the time step $\delta t \neq 1$. The diffusion model has a first-order error in δt (as well as in space), so we need the time step to be small.

Sec. II D, we will generalize our diffusion model to include both diffusion and convection.

Because the tie strength of each edge changes independently of those of the other edges, we examine the dynamics of a single edge. Let $u(x, t)$ denote the probability that the tie strength of a chosen edge at time t is given by $\exp(x)$. We write the master equation

$$u(x, t) = \frac{1}{2}[u(x - \delta x, t - \delta t) + u(x + \delta x, t - \delta t)], \quad (19)$$

which we rearrange to obtain

$$\begin{aligned} u(x, t + \delta t) - u(x, t) \\ = \frac{1}{2}\{u(x + \delta x, t) - u(x, t) - [u(x, t) - u(x - \delta x, t)]\}. \end{aligned} \quad (20)$$

We now approximate finite differences as derivatives in Eq. (20). Specifically, we take $\delta t \rightarrow 0$ and $\delta x \rightarrow 0$, while supposing that $\frac{(\delta x)^2}{\delta t}$ does not go to 0, to yield

$$\begin{aligned} \frac{\partial u}{\partial t} \delta t &= \frac{1}{2} \left[(\delta x)^2 \frac{\partial^2 u}{\partial x^2} \right] \\ \Rightarrow u_t &= \frac{1}{2} \frac{(\delta x)^2}{\delta t} u_{xx} + O(\delta x) + O(\delta t), \end{aligned} \quad (21)$$

where we use the notation $u_t \equiv \frac{\partial u}{\partial t}$ and an analogous notation for spatial derivatives. The initial condition for (21) is

$$u(x, 0) = \delta(x), \quad (22)$$

where $\delta(x)$ is the Kronecker delta function (and should not be confused with δx , which denotes an infinitesimal change in the variable x). This initial condition implies that, at time $t = 0$, the tie strength of the chosen edge is $\exp(0)$ with probability 1. Equations (21) and (22) constitute a diffusion equation with a delta-mass initial condition. With this initial condition, we can solve this equation both numerically and analytically. We define $D = \frac{1}{2} \frac{(\delta x)^2}{\delta t}$, and we obtain the similarity solution [20]

$$u(x, t) = \frac{1}{\sqrt{4\pi Dt}} \exp\left(-\frac{x^2}{4Dt}\right). \quad (23)$$

Therefore, the tie strength in the diffusion model spreads out over time as a Gaussian whose variance increases with time.

D. Bounded convection–diffusion model of tie strengths

We now modify the diffusion model in Sec. II C by supposing that there is a preference for tie strengths to grow over time. Specifically, at each time step, there is a probability of $(1/2 + \Delta)$ for a tie strength to grow by the factor $\exp(\delta x)$ and a probability of $(1/2 - \Delta)$ for it to decay by the factor $\exp(\delta x)$. We also suppose that Δ is small. We view the growth pattern of the tie strength as a one-dimensional (1D) random walker that has a preference to move in the positive direction [see Fig. 6(b)]. The associated master equation is

$$\begin{aligned} u(x, t + \delta t) &= \left(\frac{1}{2} + \Delta\right)u(x - \delta x, t) \\ &+ \left(\frac{1}{2} - \Delta\right)u(x + \delta x, t). \end{aligned} \quad (24)$$

Following a similar procedure as with the diffusion model in Sec. II C, we derive the equation

$$u_t = ku_{xx} - 4\beta ku_x + O(\delta x) + O(\delta t), \quad (25)$$

where we assume that $\frac{(\delta x)^2}{2\delta t} \rightarrow \text{const} = k$ and $\frac{\Delta}{\delta x} \rightarrow \text{const} = \beta$. We thereby obtain a convection–diffusion equation, with the delta-mass initial condition (22).

To prevent our random walker from escaping to infinity, we enforce each tie strength to have an upper bound W . Specifically,

$$u(x, t) = 0 \quad \text{for all } x > w, \quad (26)$$

where $w = \ln W$. Equation (26) is a linear diffusion equation in a moving frame. By making the change of variables $(x, t) \rightarrow (\xi, t)$, where $\xi = x - 4\beta kt$, we see that Eq. (25) becomes

$$u_t = ku_{\xi\xi}, \quad (27)$$

which is the usual diffusion equation.

Together with conservation of probability, Eq. (26) enforces a boundary condition in our scheme for our numerical computations of (25). Using a forward-time, central-difference scheme gives

$$\begin{aligned} \frac{u_j^{i+1} - u_j^i}{\delta t} &= k \frac{u_{j+1}^i - 2u_j^i + u_{j-1}^i}{(\delta x)^2} - 4\beta k \frac{u_{j+1}^i - u_{j-1}^i}{2\delta x}, \\ u_j^{i+1} &= au_{j-1}^i + bu_j^i + cu_{j+1}^i, \end{aligned} \quad (28)$$

where the superscript i indicates the time discretization, the subscript j indicates the space discretization, and

$$\begin{aligned} a &= k \frac{\delta t}{(\delta x)^2} + 2\beta k \frac{\delta t}{\delta x}, \\ b &= 1 - 2k \frac{\delta t}{(\delta x)^2}, \\ c &= k \frac{\delta t}{(\delta x)^2} - 2k\beta \frac{\delta t}{\delta x}. \end{aligned} \quad (29)$$

Inserting the expressions for k and β into (29) yields $a = \frac{1}{2} + \Delta$, $b = 0$, and $c = \frac{1}{2} - \Delta$. Inserting these values into our numerical scheme in (28) yields

$$u_j^{i+1} = \left(\frac{1}{2} + \Delta\right)u_{j-1}^i + \left(\frac{1}{2} - \Delta\right)u_{j+1}^i, \quad (30)$$

which is equivalent to Eq. (24). This indicates that the numerical scheme in Eq. (28) successfully describes the evolution of the tie strength of an edge if the tie strength is sufficiently far from the upper bound. By the minimum principle and the infinite speed of wave propagation in our linear convection–diffusion equation [20], Eqs. (25) and (27) give a nonzero solution at the boundary for any $t > 0$, but our discrete system in Eq. (24) has a nonzero solution at the boundary only after some finite time.

To implement the numerical scheme (28), we have to use a finite interval. As we discussed above, we already have an upper bound on x . We also need a lower bound. Although the solution to the convection–diffusion equation (25) has an infinite propagation speed, our discrete model has a finite propagation speed $v = \frac{\delta x}{\delta t}$. Therefore, we can choose a lower bound $-L$ (with $L \in \mathbb{R}_{>0}$) such that $L \geq \frac{T}{v}$. That is, at $t = T$, we have $u(x, T) = 0$ for all $x \leq -L$. Therefore, $u_j^i = u(x_j, t_i)$, with our space discretization given by $\{x_0 = -L, x_1, \dots, x_N = w\}$ (where $N = \frac{w+L}{\delta x}$) and our time discretization given by $\{t_0 = 0, t_1, \dots, t_{N_t} = T\}$.

We derive boundary conditions by requiring conservation of mass:

$$\sum_{j=1}^N u_j^{i+1} = \sum_{j=1}^N u_j^i. \quad (31)$$

Combining Eqs. (28) and (31) yields

$$\begin{aligned} u_1^{i+1} &= u_1^i(1-a) + u_2^i(1-a-b), \\ u_N^{i+1} &= u_N^i(1-c) + u_{N-1}^i(1-b-c). \end{aligned} \quad (32)$$

We now examine the boundary at $x = w$. From Eq. (32), the boundary condition on the right (which we derive from conservation of mass) is

$$u_N^{i+1} = \left(\frac{1}{2} + \Delta\right)u_N^i + \left(\frac{1}{2} + \Delta\right)u_{N-1}^i. \quad (33)$$

Our model requires that the tie strength of an edge does not exceed some threshold w . Therefore, whenever the tie strength of an edge reaches w , we require at the next time step that it either remains at w or decays to $w - \delta x$. Similarly, if the tie strength of an edge is w at time t , then the tie strength of that edge at time $t - \delta t$ is either $w - \delta x$ or w . If, at some time, the tie strength x is smaller than w but becomes $x + \delta x \geq w$ at the next time step, we always set the new tie strength to w . In mathematical terms, we see from this discussion that

$$\begin{aligned} u(w, t + \delta t) &= \left(\frac{1}{2} + \Delta\right)u(w, t) + \left(\frac{1}{2} + \Delta\right)u(w - \Delta x, t), \\ u_N^{i+1} &= \left(\frac{1}{2} + \Delta\right)u_N^i + \left(\frac{1}{2} + \Delta\right)u_{N-1}^i. \end{aligned} \quad (34)$$

Consequently, the natural boundary condition from the model is equivalent to the boundary condition that we impose on our numerical scheme (28) based on conservation of mass.

After choosing the bounds (i.e., the values of L and w) of the domain of u , we implement our numerical scheme (28) by building a transition matrix from Eqs. (28) and (32). This matrix is a tridiagonal matrix in which the elements of each column sum to 1, so it is a stochastic matrix and there always exists an eigenvector with eigenvalue 1. This transition matrix is a positive stochastic matrix if $\Delta < \frac{1}{2}$. By the Perron–Frobenius theorem, the eigenspace of the unit eigenvalue is spanned by one vector, which is the stationary state.

At steady state, $u(x, t) = u(x, t + \delta t)$, so it follows that $u_j^{i+1} = u_j^i$. Inserting this relation into Eq. (33) yields

$$u_N = \left(\frac{1}{2} + \Delta\right)u_{N-1} + \left(\frac{1}{2} + \Delta\right)u_N, \quad (35)$$

which implies that

$$\frac{u_N}{u_{N-1}} = \frac{\frac{1}{2} + \Delta}{\frac{1}{2} - \Delta}. \quad (36)$$

Away from the upper bound w , we have

$$\begin{aligned} u_{N-1} &= \left(\frac{1}{2} + \Delta\right)u_{N-2} + \left(\frac{1}{2} - \Delta\right)u_N \\ &= \left(\frac{1}{2} + \Delta\right)u_{N-2} + \left(\frac{1}{2} - \Delta\right)\frac{\frac{1}{2} + \Delta}{\frac{1}{2} - \Delta}u_{N-1} \\ &= \left(\frac{1}{2} + \Delta\right)u_{N-2} + \left(\frac{1}{2} + \Delta\right)u_{N-1}, \end{aligned} \quad (37)$$

which implies that

$$\frac{u_{N-1}}{u_{N-2}} = \frac{\frac{1}{2} + \Delta}{\frac{1}{2} - \Delta}. \quad (38)$$

By induction, we obtain

$$\frac{u_j}{u_{j-1}} = \frac{\frac{1}{2} + \Delta}{\frac{1}{2} - \Delta}. \quad (39)$$

From conservation of mass,

$$\int_{\mathbb{R}} u(x, t) dx = \text{const}, \quad (40)$$

which yields

$$u_x(w) = 4\beta u(w), \quad (41)$$

where we take $u \rightarrow 0$ and $u_x \rightarrow 0$ as $x \rightarrow -\infty$ based on our numerical computations. From (41), we obtain the following boundary conditions for our numerical computations:

$$\begin{aligned} \frac{u_N - u_{N-1}}{\delta x} &= 4\beta u_N, \\ u_N &= \frac{u_{N-1}}{1 - 4\Delta}. \end{aligned} \quad (42)$$

The boundary conditions in (42) are not exactly the same as those that we derived directly from the numerical conservation of mass in Eq. (31) or from the network model in Eq. (34). However, Eqs. (35) and (42) agree to first order in Δ .

Let $\eta = \frac{\frac{1}{2} - \Delta}{\frac{1}{2} + \Delta}$. From the delta-mass initial condition, we have the geometric sum

$$\begin{aligned} \sum_{j=1}^N u_j &= \frac{1}{\delta x} \\ &= u_N(1 + \eta + \eta^2 + \cdots + \eta^{N-1}) \\ &= u_N \frac{1 - \eta^N}{1 - \eta} \\ &= u_N \frac{(1 - \eta^N)(\frac{1}{2} + \Delta)}{2\Delta}. \end{aligned} \quad (43)$$

Recall that $N = \frac{w+L}{\delta x}$ and $\eta < 1$. Therefore, to obtain an asymptotic solution to (28) and (32) at steady state, we may take $\eta^N \rightarrow 0$. In this asymptotic limit, we solve for u_N in terms of Δ and β to obtain

$$u_N = \frac{2\Delta}{\left(\frac{1}{2} + \Delta\right)\delta x} = \frac{2\beta}{\left(\frac{1}{2} + \Delta\right)}. \quad (44)$$

We implement our numerical scheme in (28) and (32) with the parameter values $\delta x = 5 \times 10^{-3}$, $\delta t = 10^{-5}$, $T = 0.05$, $\beta = 15$, $w = 2$, and $\Delta = 7.5 \times 10^{-2}$. We also run 100 Monte Carlo simulations on networks from our convection–diffusion model with $n = 2000$ nodes and these same parameter values. We take a mean of the simulations and show our results in Fig. 7.

Equation (44) implies that the solution to the PDE (25) at the boundary w at stationarity does not depend on the value of w . This is pleasing, because there is no particular reason to choose one value of w over another.

The numerical scheme in (28) and (32) is accurate to first order both in time and in space. Because u_N converges to the steady-state solution $u(w)$ as we decrease δx , we can make concrete statements about the exact stationary-state solution to the convection–diffusion equation with mass-conserving

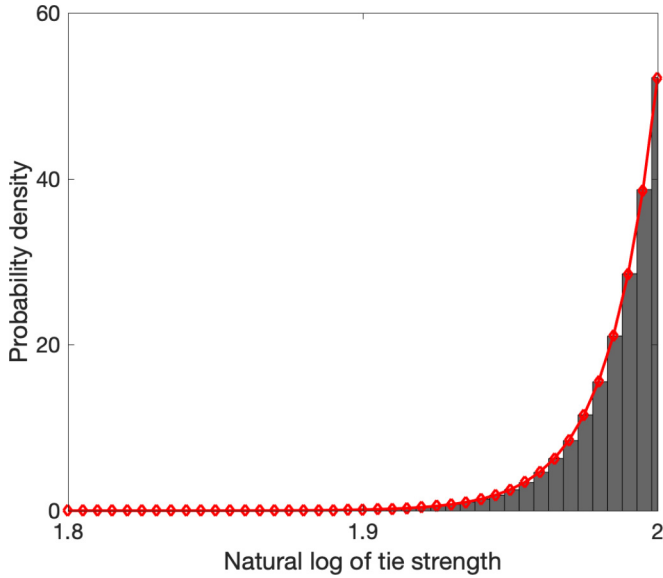


FIG. 7. Comparison of our numerical scheme (red curve) from Eqs. (28) and (32) to a mean of Monte Carlo simulations over 100 realizations of our bounded convection–diffusion network model (gray blocks). This figure gives the probability distribution of the tie strength of an edge in a network. Because we assume that each edge is independent of all other edges, this distribution applies to the tie strength of each edge in the network.

boundary conditions. The boundary value of u at stationarity is

$$u(w) = 4\beta. \tag{45}$$

From Eq. (39), we obtain the following expression for $u(x, t)$ for $x < w$ in the long-time limit (i.e., at stationarity):

$$u(x, t) = \lim_{m \rightarrow \infty} \left(\frac{\frac{1}{2} - \beta \frac{w-x}{m}}{\frac{1}{2} + \beta \frac{w-x}{m}} \right)^m 4\beta. \tag{46}$$

One can think of the expression (46) as taking the limit of our numerical scheme in (28) and (32) as the step size δx of our space discretization goes to 0. Additionally, if $u(x, t)$ is a solution to the convection–diffusion equation at stationarity, it follows that

$$\begin{aligned} \frac{u(w, t)}{u(w - \delta x, t)} &= \frac{u(w - \delta x, t)}{u(w - 2\delta x, t)} \\ &= \frac{u(w - \ell \delta x, t)}{u(w - (\ell + 1)\delta x, t)} \end{aligned} \tag{47}$$

for $\ell \in \mathbb{Z}_{\geq 0}$.

From Eq. (47), we can obtain the solution to Eq. (25) at stationarity. The solution is of the form

$$u(x) = Ce^{B(x-w)}. \tag{48}$$

We determine the constants B and C from Eqs. (40) and (45) to obtain

$$u(x) = 4\beta e^{4\beta(x-w)}. \tag{49}$$

The solution to the discrete convection–diffusion equations (28) and (32) as $\eta^N \rightarrow 0$ is

$$u_{N-j} = \frac{4\beta}{1 + 2\Delta} \eta^j, \quad j \in \{0, \dots, N\}. \tag{50}$$

Therefore, a necessary (but not sufficient) condition for our convection–diffusion network to not have a GCC is

$$\Delta < \frac{1}{4n - 2}. \tag{51}$$

The solution (49) satisfies the original convection–diffusion equation (25), subject to the conditions in Eqs. (40), (45), and (47). The formula (50) provides a way to examine the emergence of a GCC in our convection–diffusion network model in the long-time limit. At stationarity, the probability distribution of the tie strength of an edge is biased towards the boundary, so we look near the boundary $x = w$ for potentially interesting behavior. We define a threshold $W_0 < W$ and let $w_0 = \ln(W_0)$. Recall that we interpret all edges with tie strengths that are smaller than the threshold value as inactive. We interpret edges with tie strengths that are larger than or equal to the threshold as active. Assuming that the system (24) has reached stationarity, we calculate the probability that a given edge has a tie strength that is at least as large as the threshold. This probability is

$$\mathbf{P} = \frac{4\Delta}{1 + 2\Delta} \frac{1 - \eta^{k+1}}{1 - \eta}, \tag{52}$$

where $k = \lfloor \frac{w-w_0}{\delta x} \rfloor$. When $\mathbf{P} > 1/n$, our network has a GCC with high probability. A phase transition occurs when $\mathbf{P} = 1/n$.

One can also study the stationary states of the convection–diffusion equation (25) directly by setting $u_t = 0$ to obtain an ordinary differential equation. This gives the same result as Eq. (49), provided we use the same initial and boundary conditions.

Another way to look at the growth and decay of tie strengths in our convection–diffusion network model is by identifying the growth-and-decay process as a 1D birth–death Markov process [21]. However, to use such an approach, we need the process to have a state space Ω that is not bounded from below. A way to do this is to first examine a finite state space and then take the limit as its lower bound goes to negative infinity. Examining a 1D birth–death Markov process gives another way to derive Eq. (39).

An advantage of analyzing our tie-decay temporal network model using ideas from convection–diffusion equations is that it allows us to write down a characteristic time scale for a network to reach a stationary state. From Eq. (27), we can view the convection–diffusion equation as a diffusion equation in a moving frame. Let τ_1 to be the time that it takes for the initial configuration to move to the boundary at $x = w$. This time is given by

$$\tau_1 = \frac{w}{4\beta k}.$$

Because the solution (23) to the diffusion equation is a Gaussian distribution that expands over time, we define τ_2 to be the time that it takes for the initial configuration to expand until it

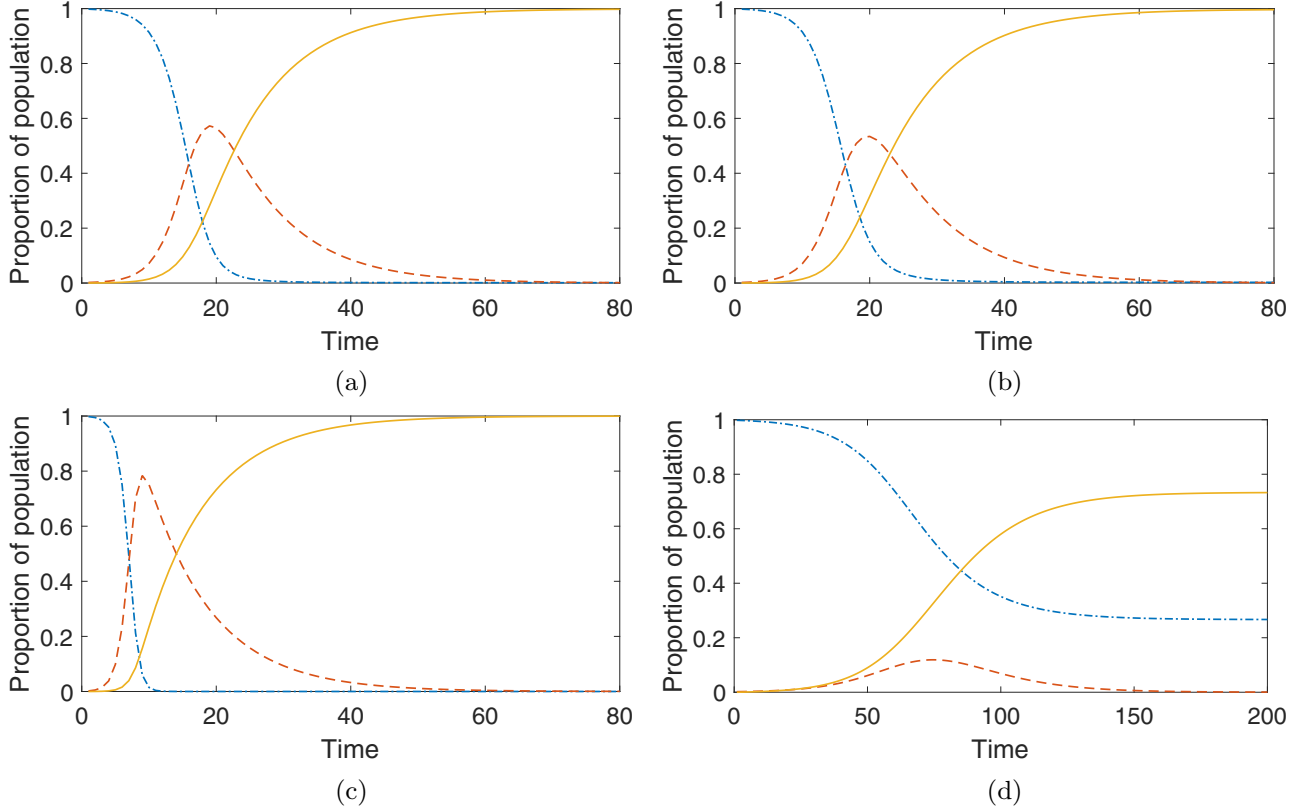


FIG. 8. Comparison of (a) the discrete SIR model (54) and (b)–(d) SIR disease spread on simplified back-to-unity tie-decay networks with different values of $\lambda = N_p \mathbf{P}$, where N_p is the population and \mathbf{P} is the probability that a tie strength is larger than or equal to the threshold. We show the fractions of the population in each state (i.e., compartment) as a function of time for (b) $\lambda = 1$, (c) $\lambda = 3$, and (d) $\lambda = 0.3$. In each panel, the horizontal axis is time, the dot-dashed blue curve indicates susceptible individuals, the dashed red curve indicates infected individuals, and the solid yellow curve indicates recovered individuals. The infection rate is $\bar{\beta} = 0.6$, the recovery rate is $\bar{\gamma} = 0.1$, and the population is $N_p = 5000$. Our initial conditions are $S(0)/N_p = 0.998$, $I(0)/N_p = 0.002$, and $R(0) = 0$. Observe the similarity between the plots in panels (a) and (b).

has a standard deviation of w . This time is given by

$$\tau_2 = \frac{w^2}{2k}.$$

Therefore, we expect to reach stationarity at roughly $\tau = \max\{\tau_1, \tau_2\}$ when starting from a delta mass initial condition. This characterization of τ is similar to determining a time scale based on the Péclet number [22], which measures the relative strengths of convection and diffusion. If we use w as length scale, the Péclet number is $\text{Pe} = 4\beta w$. Additionally, $\tau = \tau_2$ if and only if $\tau_2 \geq \tau_1$; equivalently, $\tau = \tau_2$ if and only if $2\beta w \geq 1$, which entails that $\text{Pe} \geq 2$.

III. APPLICATION: A COMPARTMENTAL MODEL OF AN INFECTIOUS DISEASE ON A TIE-DECAY NETWORK

Many infectious diseases spread in humans through networks of contacts between susceptible and infected people [18,23]. However, not all contacts between infected and susceptible people result in an infection. If we are given the interaction pattern between individuals, we can calculate the associated tie strength of different pairs of people as a function of time. By setting a threshold on the tie strength, suppose that only contacts whose tie strength is at least as large as

the threshold result in a new infection. In this section, we use a tie-decay network for the interaction patterns between individuals and simulate a compartmental model on such a network. We consider an SIR contagion [24,25]. [See [26] for an investigation of susceptible–infected–susceptible (SIS) contagions on tie-decay networks.] Suppose for simplicity that individuals in a population interact with each other according to the simplified back-to-unity model of Sec. II B. This assumption requires that each pair of individuals interact with equal probability. In reality, interaction probabilities are heterogeneous, and such heterogeneity can significantly affect the spread of a disease [18,23]. We also assume that the spread of the disease does not affect the interactions in a network. This assumption is also unrealistic, although it can be reasonable in situations such as the early stages of an epidemic. The spread of an infectious disease depends on how much and how frequently individuals interact with each other. We also assume that the tie-decay network has already reached a stationary state when the disease first enters the population, so we can use the distribution (17) of the tie strengths of the network at stationarity.

We follow common notation for SIR models [25]. Suppose that the population size is N_p . Let $S(t)$, $I(t)$, and $R(t)$ denote the (time-dependent) numbers of individuals in the suscepti-

ble, infected, and recovered compartments, respectively. The continuous-time SIR model in a well-mixed population is

$$\begin{aligned} \frac{dS}{dt} &= -\bar{\beta}IS/N_p, \\ \frac{dI}{dt} &= \bar{\beta}IS/N_p - \bar{\gamma}I, \\ \frac{dR}{dt} &= \bar{\gamma}I, \end{aligned} \tag{53}$$

where $\bar{\beta}$ is the infection rate and $\bar{\gamma}$ is the recovery rate. Because it is easier to track the number of people in each compartment on a daily or weekly basis than in continuous time, it is often more meaningful to consider the following discrete version of the SIR model:

$$\begin{aligned} S_{i+1} &= S_i - \bar{\beta}I_iS_i/N_p, \\ I_{i+1} &= I_i + \bar{\beta}I_iS_i/N_p - \bar{\gamma}I_i, \\ R_{i+1} &= R_i + \bar{\gamma}I_i. \end{aligned} \tag{54}$$

One interpretation of the term $\bar{\beta}I_iS_i/N_p$ is as follows. In one time step, we suppose that each susceptible individual interacts with a person who we select uniformly at random from a population. With probability I/N_p , this person is in the infected compartment. An interaction between a susceptible person and an infected person results in the former becoming infected with probability $\bar{\beta}$. The SIR models (53) and (54) assume that disease spread does not affect the interaction patterns of individuals.

In the synchronous-updating SIR model (54), each individual from the susceptible compartment interacts with one person in a single time step. By contrast, in the SIR model that we examine on a tie-decay network, we assume that each individual from the susceptible compartment interacts with anyone in the population with the same probability p . The only active interactions are ones with tie strengths that are at least as large as the threshold. The probability \mathbf{P} that a tie strength is larger than or equal to the threshold is given by Eq. (17). In a back-to-unity tie-decay network, in one time step, an individual from the susceptible compartment can have active interactions with any other individual in the population with a probability that is given by Eq. (17). Therefore, the number of active interactions of a susceptible person satisfies a Poisson distribution, with mean $\lambda = N_p\mathbf{P}$, when the population N_p is large and \mathbf{P} is small. In summary, we describe SIR disease spreading on a tie-decay network as follows. We have a population of size N_p . An individual in the susceptible compartment can have active interactions with each other individual in the population with a homogeneous, independent probability \mathbf{P} . An active interaction between a susceptible person and an infected person leads to infection with probability $\bar{\beta}$, and people from the infected compartment recover at rate $\bar{\gamma}$.

We compare the results of simulating Eq. (54) and SIR disease spreading on simplified back-to-unity tie-decay networks for several values of λ in Fig. 8. When $\lambda = 1$, we see that the discrete SIR model (54) is a good approximation for SIR disease spreading on such a tie-decay network. However, when $\lambda > 1$, each susceptible individual interacts on average with more than one person in each time step, so the disease

spreads faster on the tie-decay network than in (54). When $\lambda < 1$, a susceptible individual interacts on average with fewer than one person in each time step, so the disease spreads more slowly on the tie-decay network than in (54). We also note that $\lambda > 1$ corresponds to the criterion for the existence of a GCC (with high probability) in our simplified back-to-unity tie-decay network model as $N_p \rightarrow \infty$. Therefore, we see that when there is a GCC in a back-to-unity tie-decay network, an SIR contagion tends to spread faster than in the discrete SIR model (54). When there is no GCC in such a tie-decay network, an SIR contagion tends to spread more slowly than in the discrete SIR model (54).

IV. CONCLUSIONS AND DISCUSSION

It is very popular to study temporal networks [3–5], but most investigations of such networks focus on discrete-time approaches. However, many networks evolve continuously in time, and it is important to develop approaches for studying such temporal networks. This is an important modeling consideration, and it is often useful to consider the underlying time as continuous even when subsequently discretizing the dynamics of temporal networks.

In the present paper, we studied several continuous-time network models with tie decay. We investigated the long-time behavior of these models and examined the emergence of giant connected components (GCCs) in the long-time limit in the networks that these models produce. In addition to exploring two existing continuous-time models—the tie-decay model of Ahmad *et al.* [6] and a simplified version of the back-to-unity model of Jin *et al.* [12]—we also developed a diffusion model and a convection–diffusion model for tie strengths, and we examined the formation of a GCC in the latter (which is a generalization of the former). We derived the stationary distribution of tie strengths in the convection–diffusion model using intuition from numerical computations of a linear convection–diffusion PDE. Our analytical results agree with our numerical simulations in the long-time limit. We also examined SIR contagions on networks that we constructed using the simplified back-to-unity model.

All of the models that we studied in the present paper produce temporal networks in which we distinguish between interactions and ties between nodes. In all of these models, the tie strength between two nodes grows when they interact and decays exponentially when they do not. The specific way in which tie strengths change is a key difference between the models. In the tie-decay model of [6], the tie strength between two nodes grows by 1 when there is an interaction between them. In the back-to-unity model of [12], the tie strength between two nodes becomes 1 when they interact. In the diffusion model and the convection–diffusion model, the tie strength experiences instantaneous exponential growth when there is an interaction. Another way in which the models differ is in the time scale between the interactions between two given nodes. In the Ahmad *et al.* tie-decay model [6] and the back-to-unity model [12], it is rare for two given nodes to interact with each other in a given time step. Therefore, on average, the strength of a tie between two nodes decays for a long time after each interaction between them. By contrast, in the bounded convection–diffusion model of tie strengths of

Sec. IID, the probabilities of having an interaction (namely, $\frac{1}{2} + \Delta$) and of not having an interaction (namely, $\frac{1}{2} - \Delta$) are both close to 1/2, with the former slightly larger than the latter. (In the diffusion model of Sec. IIC, these probabilities are exactly 1/2.) Consequently, the tie strength between two nodes does not decay for much time before there is another interaction between them. In this model, we also impose an upper bound on tie strengths to prevent them from becoming arbitrarily large.

The tie-decay model of Ahmad *et al.* [6] and the back-to-unity model [12] are interesting models of interactions between people (or other entities) that are worth exploring in applications. In Sec. III, we examined SIR contagions on networks that are produced by a simplified back-to-unity model. Using these types of models allows one to incorporate a variety of interaction patterns, and it is important to further study how different patterns affect dynamical processes on social networks. Current efforts include investigations of SIS contagions [26] and opinion dynamics [27] on the tie-decay networks of Ahmad *et al.* [6]. Given that the tie strength between two neurons can increase when they have similar

interaction patterns [11], we also expect network models like the ones that we studied in the present paper to be relevant for the analysis of phenomena like Hebbian learning in neuronal systems.

When generalizing network analysis to continuous-time formulations of temporal networks, it is useful to adapt familiar network ideas. Important notions to adapt include random-graph models and GCCs (as in the present paper), and it will be valuable to focus future efforts on generalizing other ideas (such as community structure and various dynamical processes on networks) to continuous-time network models. In our analysis, we treated edges as evolving independently, but many systems have correlations (e.g., mutual excitation or mutual inhibition) between edges, and it is important to generalize our analysis for those situations and to study how such correlations affect dynamical processes.

ACKNOWLEDGEMENTS

We thank Mariano Beguerisse-Díaz, Heather Zinn Brooks, Tom Chou, and Hanbaek Lyu for helpful discussions.

-
- [1] M. E. J. Newman, *Networks*, 2nd ed. (Oxford University Press, Oxford, UK, 2018).
- [2] M. A. Porter, Nonlinearity + networks: A 2020 vision, in *Emerging Frontiers in Nonlinear Science*, edited by P. G. Kevrekidis, J. Cuevas-Maraver, and A. Saxena (Springer International Publishing, Cham, Switzerland, 2020), pp. 131–159.
- [3] P. Holme and J. Saramäki, Temporal networks, *Phys. Rep.* **519**, 97 (2012).
- [4] P. Holme, Modern temporal network theory: A colloquium, *Eur. Phys. J. B* **88**, 234 (2015).
- [5] P. Holme and J. Saramäki, *Temporal Network Theory* (Springer International Publishing, Cham, Switzerland, 2019).
- [6] W. Ahmad, M. A. Porter, and M. Beguerisse-Díaz, Tie-decay temporal networks in continuous time and eigenvector-based centralities, [arXiv:1805.00193](https://arxiv.org/abs/1805.00193).
- [7] R. S. Burt, Decay functions, *Social Networks* **22**, 1 (2000).
- [8] K. Lerman, Information is not a virus, and other consequences of human cognitive limits, *Future Internet* **8**, 21 (2016).
- [9] K. Lerman, R. Ghosh, and T. Surachawala, Social contagion: An empirical study of information spread on Digg and Twitter follower graphs, [arXiv:1202.3162](https://arxiv.org/abs/1202.3162).
- [10] H. Navarro, G. Miritello, A. Canales, and E. Moro, Temporal patterns behind the strength of persistent ties, *EPJ Data Sci.* **6**, 31 (2017).
- [11] E. Agliari and A. Barra, A Hebbian approach to complex-network generation, *Europhys. Lett.* **94**, 10002 (2011).
- [12] E. M. Jin, M. Girvan, and M. E. J. Newman, Structure of growing social networks, *Phys. Rev. E* **64**, 046132 (2001).
- [13] C. Fritz, M. Lebacher, and G. Kauermann, Tempus volat, hora fugit: A survey of dynamic network models in discrete and continuous time, *Statistica Neerlandica* **74**, 275 (2020).
- [14] R. Sulo, T. Berger-Wolf, and R. Grossman, Meaningful selection of temporal resolution for dynamic networks, in *MLG '10: Proceedings of the Eighth Workshop on Mining and Learning with Graphs* (Association for Computing Machinery, New York, NY, USA, 2010), pp. 127–136.
- [15] P. Erdős and A. Rényi, On the evolution of random graphs, *Public. Math. Inst. Hung. Acad. Sci.* **5**, 17 (1960).
- [16] A. A. Saberi, Recent advances in percolation theory and its applications, *Phys. Rep.* **578**, 1 (2015).
- [17] E. López, R. Parshani, R. Cohen, S. Carmi, and S. Havlin, Limited Path Percolation in Complex Networks, *Phys. Rev. Lett.* **99**, 188701 (2007).
- [18] R. Pastor-Satorras, C. Castellano, P. Van Mieghem, and A. Vespignani, Epidemic processes in complex networks, *Rev. Mod. Phys.* **87**, 925 (2015).
- [19] D. F. Gleich, PageRank beyond the Web, *SIAM Rev.* **57**, 321 (2015).
- [20] L. C. Evans, *Partial Differential Equations*, 2nd ed., Graduate Studies in Mathematics Vol. 19 (American Mathematical Society, Providence, RI, USA, 2010).
- [21] D. A. Levin and Y. Peres, *Markov Chains and Mixing Times* (American Mathematical Society, Providence, RI, USA, 2017).
- [22] G. K. Batchelor, *An Introduction to Fluid Dynamics* (Cambridge University Press, Cambridge, UK, 1967).
- [23] I. Z. Kiss, J. C. Miller, and P. L. Simon, *Mathematics of Epidemics on Networks: From Exact to Approximate Models* (Springer International Publishing, Cham, Switzerland, 2017).
- [24] W. O. Kermack and A. G. McKendrick, A contribution to the mathematical theory of epidemics, *Proc. R. Soc. A* **115**, 700 (1927).
- [25] F. Brauer, C. Castillo-Chavez, and Z. Feng, *Mathematical Models in Epidemiology* (Springer-Verlag, Heidelberg, Germany, 2019).
- [26] Q. Chen and M. A. Porter, Epidemic thresholds of infectious diseases on tie-decay networks, [arXiv:2009.12932](https://arxiv.org/abs/2009.12932).
- [27] K. Sugishita, M. A. Porter, M. Beguerisse-Díaz, and N. Masuda, Opinion dynamics in tie-decay networks, [arXiv:2010.00143](https://arxiv.org/abs/2010.00143).

Correction: A minor error in Eq. (5) has been fixed.